Photosynthesis Research (2022) 154:113–124
https://doi.org/10.1007/s11120-022-00951-6

ORIGINAL ARTICLE

Biochemical and spectroscopic characterizations of the oligomeric antenna of the coral symbiotic Symbiodiniaceae *Fugacium kawagutii*

Dariusz M. Niedzwiedzki[1,2] · Nikki Cecil M. Magdaong[3] · Xinyang Su[4] · Haijun Liu[4]

Received: 19 May 2022 / Accepted: 16 August 2022 / Published online: 7 September 2022

Abstract

Light-harvesting antennas in photosynthesis capture light energy and transfer it to the reaction centers (RCs) where photochemistry takes place. The sustainable growth of the reef-building corals relies on a constant supply of the photosynthates produced by the endosymbiotic dinoflagellate, belonging to the family of *Symbiodiniaceae*. The antenna system in this group consists of the water-soluble peridinin-chlorophyll *a*-protein (PCP) and the intrinsic membrane chlorophyll *a*-chlorophyll c_2-peridinin protein complex (acpPC). In this report, a nonameric acpPC is reported in a dinoflagellate, *Fugasium kawagutii* (formerly *Symbiodinium kawagutii* sp. CS-156). We found that extensive biochemical purification altered the oligomerization states of the initially isolated nonameric acpPC. The excitation energy transfer pathways in the acpPC nonamer and its variants were studied using time-resolved fluorescence and time-resolved absorption spectroscopic techniques at 77 K. Compared to the well-characterized trimeric acpPC, the nonameric acpPC contains an 11 nm red-shifted terminal energy emitter and substantially altered excited state lifetimes of Chl *a*. The observed energetic overlap of the fluorescence terminal energy emitters with the absorption of RCs is hypothesized to enable efficient downhill excitation energy transfer. Additionally, the shortened Chl *a* fluorescence decay lifetime in the oligomeric acpPC indicate a protective self-relaxation strategy. We propose that the highly-oligomerized acpPC nonamer represents an intact functional unit in the *Symbiodiniaceae* thylakoid membrane. They perform efficient excitation energy transfer (to RCs), and are under manageable regulations in favor of photoprotection.

Keywords LHC · Symbiodiniaceae · acpPC · Oligomer · Transient absorption · Time-resolved fluorescence

Introduction

Photosynthesis is a process in which light energy is harvested and converted to chemical energy to sustain life and evolution. Two of the early events in photosynthesis, i.e., light capture and photochemical conversion, are accomplished by two types of pigmented-protein complexes (PPCs): light-harvesting antenna complexes (LHCs), which are responsible for photon absorption and transfer of the excitation energy, and the reaction centers (RCs), where primary photochemistry occurs. Compared to the relatively conserved RCs, a variety of light-harvesting complexes has evolved to match the photosynthetic organisms' eco-physiological niche (Blankenship 2002).

Dinoflagellates in the family of *Symbiodiniaceae* are important photosynthetic symbionts in cnidarians (such as corals) and other coral reef organisms. They have evolved two unique types of LHCs: the peridinin-chlorophyll *a*-protein (PCP) and the chlorophyll *a*-chlorophyll c_2-peridinin-protein complex (acpPC) (Hiller et al. 1993, 1995; Hofmann et al. 1996; Sharples et al. 1996; Schulte et al. 2009a, b; Schulte et al. 2010). PCP is a water-soluble complex residing in the thylakoid lumen. PCP contains peridinin, a structurally complex carotenoid, as a primary photosynthetic pigment, which, upon excitation, transfers the energy to chlorophyll *a* (Chl *a*). Structural and spectroscopic studies of PCP have greatly advanced

✉ Dariusz M. Niedzwiedzki
niedzwiedzki@wustl.edu

✉ Haijun Liu
liuhaijun@wustl.edu

1 Center for Solar Energy and Energy Storage, Washington University in St. Louis, St. Louis, MO 63130, USA

2 Department of Energy Environmental and Chemical Engineering, Washington University in St. Louis, St. Louis, MO 63130, USA

3 Department of Chemistry, Washington University in St. Louis, St. Louis, MO 63130, USA

4 Department of Biology, Washington University in St. Louis, St. Louis, MO 63130, USA

our understanding of this antenna complex (Hofmann et al. 1996; Zigmantas et al. 2002; Ilagan et al. 2006; Schulte et al. 2009a, b; van Stokkum et al. 2009; Niedzwiedzki et al. 2013). However, it remains unclear how the membrane extrinsic PCP interacts with the thylakoid membrane and what the route is of the excitation energy migration from PCP to the RCs (Reynolds et al. 2008; Kanazawa et al. 2014).

AcpPC in *Symbiodiniaceae* is an intrinsic membrane protein complex, belonging to the LHC protein superfamily (Durnford et al. 1999). In comparison to PCP, acpPC has much higher abundance in the algal cells (Iglesias-Prieto et al. 1991). It was revealed that acpPC consists of a group of polypeptides with molecular weight (MW) of 18–20 kDa. Spectroscopic studies indicated that both peridinin and Chl c_2 pigments transfer excitations to Chl *a*. It was postulated that the excitation energy transfer pathways involve the peridinin S_2 electronic excited state and S_1/ICT (intramolecular charge-transfer) states. The inter-pigment energy transfer yields are high, close to unity. The role of another carotenoid, diadinoxanthin, found in the antenna complex, is still unclear (Polivka et al. 2006, Di Valentin et al. 2010; Slouf et al. 2013; Niedzwiedzki et al. 2014). As aforementioned, acpPC has been the subject of research using various molecular spectroscopic techniques, investigations on the possible oligomerization states and their relationships to the pigments' energetic landscape in acpPC, however, are scarce. Our previous study provided the first evidence that the functional state of acpPC is a trimer (Jiang et al. 2014), in analogy to other LHC superfamily proteins from photosynthetic eukaryotes (Liu et al. 2004; Buchel 2015). It remains unclear, however, if there exist any higher order oligomerization states of acpPC. If yes, how they are functionally and structurally different than the well-characterized trimeric acpPC.

In this study, we report two acpPC samples with apparently different higher-order oligomeric organizations and their subsequent spectroscopic characterizations. This study also showcases that the oligomerization states of the acpPC complex can be altered, and the pigment content decreases upon further biochemical processing. Through the applications of time-resolved absorption and fluorescence emission spectroscopies performed at 77 K, we have studied whether alterations of the oligomerization states of acpPC affect excitation energy transfer.

Materials and methods

Algal culture and isolation of acpPC protein

Fugacium kawagutii (formerly *Symbiodinium kawagutii* sp. CS-156 cells) cells were cultured in f/2 media under diurnal cycle (14 h:10 h of light: dark) at 25 °C. Briefly, Guillard's (f/2) marine water enrichment solution (Sigma-Aldrich, St. Louis, MO) was diluted in filtered, sterile seawater to achieve the reconstituted growth media. Illumination was provided by an array of white colored fluorescent lamps at an intensity of 50 µmol photons·m^{-2} s^{-1}. The culture in late exponential growth phase (after 3–4 weeks) was harvested by centrifugation at 6000 rpm using Sorvall SLC-6000 centrifuge bottles at 4 °C. Cell pellets were resuspended in MMB buffer containing 20 mM 2-morpholinoethanesulfonic acid (MES) at pH 6.3, 5 mM $MgCl_2$, and 1 M betaine, and saved in − 80 °C until ready to use. Subsequently, cells were disrupted by passing twice through French press, with the French press cell prechilled at 4 °C, at 8×10^7 Pa, and a protease inhibitor cocktail (A32965, Pierce, Thermo-Fisher Scientific, Waltham, MA) and deoxyribonuclease (DN25-1G, Sigma-Aldrich, St. Louis, MO) added and completely dissolved. The cell lysate was centrifuged at 2000×*g* for 5 min to dispose the unbroken cells, and the supernatant was then centrifuged at 100,000×*g* for 30 min to collect the thylakoid membrane particles. The pellet was then resuspended and homogenized with a paintbrush in MBNC buffer containing 20 mM MES at pH 6.3, 1 M betaine, 10 mM NaCl, and 5 mM $CaCl_2$ to a Chl *a* concentration of 1.0 mg/mL. The membranes were then solubilized to a 1% (v/v) *n*-dodecyl-β-D-maltopyranoside (β-DDM) final concentration, for 15 min in the dark with gentle stirring. In the next step, the sample was centrifuged at 30,000×*g* for 20 min to remove the insoluble debris, and the supernatant was then loaded onto the sucrose density step gradient (SDG) ultracentrifugation tubes containing 0.1, 0.4, 0.7, 1.0, 1.3 M sucrose in 25 mM HEPES buffer (pH 7.0, 1 M betaine, 0.04% β-DDM). After centrifugation at 160,000×*g* for 18 h, the bands containing the acpPC fraction (SDG-acpPC) were collected for purity and spectroscopic analysis. Collected SDG-acpPC sample was further purified using ion exchange chromatography (IEC) (HiTrap Q HP column, Sigma-Aldrich, St. Louis, MO) with BioLogic DuoFlow Medium-Pressure Chromatography Systems (Bio-Rad, Hercules, CA). Linear gradient of NaCl from 15 to 200 mM in MBNC buffer was used to elute the sample. Protein samples were desalted and concentrated using 100 kDa MWCO Amicon Ultra-15 centrifugal filters (Millipore-Sigma, St. Louis, MO). The flow-through was further desalted and concentrated using Ultra-15 centrifugal filters (30 kDa MWCO, Millipore-Sigma, St. Louis, MO) and was named SDG-IEC^{FT}. Determination of acpPC protein oligomerization states in SDG, SDG-IEC and SDG-IEC^{FT} preparations was performed using blue native gel (Schagger and von Jagow 1991).

Pigment analysis of acpPC

The pigment composition of the initial complex (SDG-acpPC) was determined using high performance liquid chromatography (HPLC, Agilent, Santa Clara, CA).

Pigments were extracted from an aliquot (~ 25 µL) of the band collected after SDG ultracentrifugation (Fig. 1a) by mixing the sample with methanol. The mixture was vortexed for a few seconds, followed by centrifugation at 9400×*g* for 1 min. The supernatant was carefully collected and dried under N_2 air on ice and dim light. The dried extract was then resuspended with 100 µL of methanol/acedonitrile (70:30 v/v), filtered and injected into an Agilent HPLC Series 1100 equipped with a Zorbax Eclipse XDB C18 column. The flow rate of the mobile phase was set to 1 mL/min, starting with an isocratic flow of 99% Solvent A (87:10:3 v/v/v acetonitrile/methanol/water) and 1% Solvent B (100% ethyl acetate) for 15 min, followed by a linear gradient to 40 min to a solvent composition of 60% Solvent A and 40% Solvent B. Data were collected and analyzed using Agilent Openlab CDS Chemstation software.

Femtosecond time-resolved transient absorption spectroscopy

Time-resolved pump-probe transient absorption (TA) experiments were carried out using Helios, a femtosecond TA spectrometer (Ultrafast Systems, Sarasota, FL) coupled to a femtosecond laser system previously described in detail (Niedzwiedzki et al. 2011). The acpPC sample was excited at 540 nm, preferentially corresponding to the peridinin absorption. The energy of the pump beam was set to 200 nJ in a spot size of 1 mm diameter corresponding to a laser flux of ~ 10^{14} photons ·cm^{-2}.

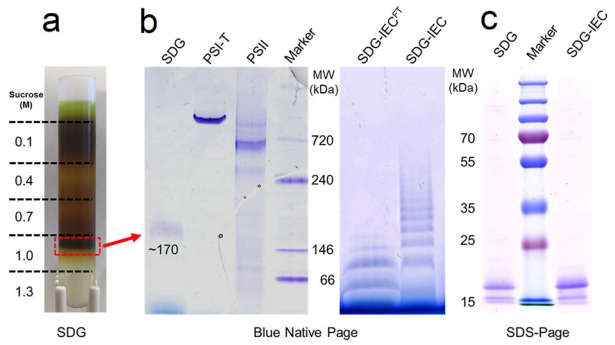

Fig. 1 Separation and biochemical characterizations of oligomeric form of acpPC antenna from *Fugacium kawagutii*. **a** SDG separation of solubilized thylakoid membrane. Sucrose concentration (M) of each step is labelled. Red square (dashed line) indicated sample is subjected for analysis. **b** Blue native PAGE analysis of the most intense band loaded directly after centrifugation (SDG, left panel) or after additional purification with ion exchange chromatography and subsequent concentration using 100 kDa (MWCO) filtration (SDG-IEC, right panel). The flowthrough (FT) from 100 kDa ultrafiltration was further concentrated using 30 kDa (MWCO) filtration, the retentate is denoted as SDG-IEF^{FT}, but not subjected for further analysis. SDG reveals single band with MW of ~ 170 kDa. Further processing of the band through IEC/ultrafiltration altered the original oligomeric state resulting in several oligomeric forms as indicated by a ladder-like band pattern. (c) SDS-PAGE analysis of SDG- and SDG-IEC-acpPC. *PSII*—photosystem II from a cyanobacterium, *Synechocystis sp*. PCC 6803, *PSI-T*—photosystem I trimer from *Synechocystis sp*. PCC 6803, *MW*—molecular weight, *SDG*—sucrose density gradient, *SDS*—sodium dodecyl sulfate

Time-resolved fluorescence spectroscopy

Time-resolved fluorescence (TRF) experiments were carried out using a Hamamatsu universal streak camera consisting of a cooled N51716-04 streak tube, C5680 blanking unit, digital CCD camera (Orca2), slow speed M5677 unit, C10647 and C1097-05 delay generators and an A6365-01 spectrograph from Bruker. Excitation pulses at 540 nm were produced by an ultrafast optical parametric oscillator (OPO) Inspire100 (Spectra-Physics, Milpitas, CA) pumped with a Mai-Tai ultrafast Ti:Sapphire laser (Spectra-Physics, Milpitas, CA), generating ~ 90 fs laser pulses at 820 nm with a frequency of 80 MHz. After OPO, the frequency of excitation beam was lowered to 4 MHz (250 ns between subsequent excitations) by 3980 Pulse Selector equipped with 3986 controller (Spectra-Physics, Milpitas, CA). Excitation beam with power of ~ 10 mW was focused on the sample in a circular spot of 2 mm diameter which corresponds to ~ 10^{10} photons·cm^{-2}.

Spectroscopic data processing and global analysis

Surface Xplorer 4 (Ultrafast Systems, Sarasota, FL) was used to correct for the dispersion present in the TA data. Global fitting of TRF and TA datasets was performed using CarpetView (Light Conversion, Vilnius, Lithuania) with so-called target modeling that uses anticipated kinetic models (van Stokkum et al. 2004), The fitting included convolution of the data with Gaussian-like instrument response function having a full width at half maximum of ~ 200 fs for Helios (TA) and ~ 0.35 ns for streak camera setup (TRF). All plots were done in Origin 2021b (Origin Lab Corp., Northampton, MA).

Results

Oligomeric states of acpPC

The isolated acpPC complex from *Fugacium kawagutii* is evidently different than the one previously reported (Polivka et al. 2006, Slouf et al. 2013; Jiang et al. 2014). For the current preparation, the thylakoid membranes were initially solubilized by β-DDM in the presence of 1 M betaine and then subjected to SDG ultracentrifugation, resulting in three major bands (Fig. 1a). We proceeded with the most abundant fraction (marked with a red rectangle) for further analysis.

The functional acpPC has been previously identified as a trimer with molecular weight (MW) of 66.5 kDa and the apo-peptide subunit of 18.3 kDa (Jiang et al. 2014). Our current preparation, however, represents a novel oligomerization state of acpPC, with MW of 170–180 kDa as estimated using Blue Native gel (BN-gel) analysis (Fig. 1b, SDG). The BN-gel is usually employed to estimate MW and the oligomerization states of the native protein complexes provided the MW of the base subunit is known (Schagger and von Jagow 1991). Note that there is no indication of any presence of photosystems (PSI, PSII) associated with this band. The SDS-PAGE analysis of the acpPC complex (Fig. 1c) indicates the MW of the major band as 18 kDa with some microheterogeneity, which seems consistent with our previous report on the same species (Jiang et al. 2014). Therefore, the SDG-acpPC sample was assigned to be a nonamer, most likely a trimer of the previously characterized trimeric acpPC ($acpPC^{3\times3}$ vs $acpPC^{3}$) (Jiang et al. 2014). Interestingly, BN-gel analysis on the sample SDG-IEC-acpPC, Fig. 1b right panel) reveals that the nonamer may have broken down and then reaggregated (reassembled), forming a ladder-like appearance of multiple bands with MW consisting of subunit multiples (Fig. 1a, b, SDG vs. SDG-IEC vs. SDG-IEC^{FT}). Protein subunit analysis (SDS-PAGE) on the SDG-acpPC and SDG-IEC-acpPC did not detect any compositional difference. Apparently, further purification of the SDG-acpPC using IEC and subsequent ultrafiltration altered the nonameric state of the SDG-acpPC and triggered the formation of a mixture of numerous oligomers (Fig. 1b). The 100-kDa filter (MWCO) flowthrough of the SDG-IEC sample was collected and further concentrated using 30 kDa filter. The oligomerization states of the sample were analyzed (Fig. 1b, SDG-IEC^{FT}), but was not subjected for further spectroscopic analysis.

Steady-state absorption and fluorescence emission

To address whether the disassembly and then reassembly (reaggregation) of acpPC (Fig. 1b, right panel) is associated with any loss of the pigments, the pigment compositions of SDG-acpPC and SDG-IEC-acpPC were compared. Firstly, the pigment content was determined using HPLC equipped with photodiode array (Fig. S1). This analysis showed that the pigment contents remain unchanged compared to those of the trimeric acpPC. Note, pigments' identification was done according to their elution times and absorption spectra, which seems, respectively, consistent with our previous studies (Niedzwiedzki et al. 2014). Subsequently, to find out if any pigments are lost between SDG-acpPC and SDG-IEC-acpPC, a basic spectral analysis of absorption spectra of both preparations was performed. This subject was better evaluated by taking absorption spectra at 77 K, since cryogenic temperature enhances spectral differences. The spectra are shown in Fig. 2a. The black spectrum corresponds to the oligomeric (nonamer) acpPC complex, and the blue spectrum corresponds to the same batch sample which was additionally purified using IEC and then concentrated (SDG-IEC-acpPC). The spectral normalization at 590 nm was under the assumption that sample absorbance at this wavelength should be least affected by further purification. The band around 590 nm is mostly associated with absorption of Chl c_2 and therefore, we tentatively assumed that stoichiometry of this pigment does not change between preparations. Such expectation originates from the fact that pigment arrangements in the structure of the monomeric

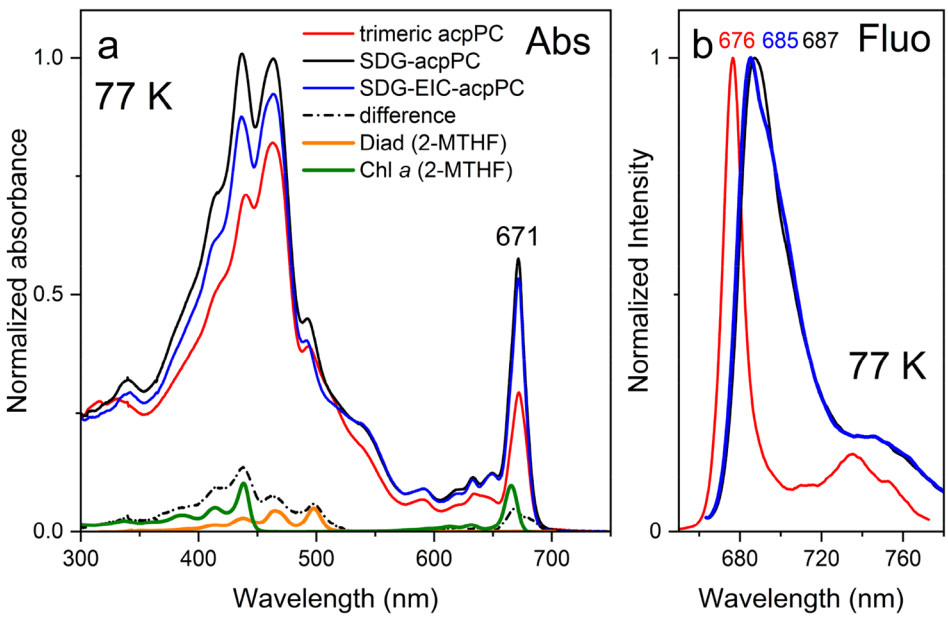

Fig. 2 **a** 77 K steady-state absorption (Abs) and **b** fluorescence emission (Fluo) spectra of trimeric and oligomeric forms (SDG-acpPC, SDG-IEC-acpPC) of the acpPC complex from *Fugacium kawagutii*. The absorption spectra are normalized at 590 nm upon assumption that Chl c_2 content will be minimally affected by post-SDG purification/processing. Difference spectrum (red dash-dot, SDG-minus-SDG-IEC) shows that further sample processing removes some fraction of Chl *a* and diadinoxanthin (Diad). The difference spectrum is very similar to the sum of the reference spectra of both pigments taken in 2-MTHF at 77 K (spectrally shifted to match peak positions)

acpPC of this species could be similar to the one recently revealed in the FCP complex from the diatom *Phaeodactylum tricornutum* (Wang et al. 2019). The FCP complex shows significantly high similarity in its pigment content to the acpPC, however, instead of peridinin it binds the carotenoid fucoxanthin. The structure of FCP monomer shows two molecules of Chl c_2 centrally bound in the complex, surrounded by a layer of multiple Chls *a* and fucoxanthins and one peripherally-bound diadinoxanthin. If such Chl c_2 binding chemistry is conserved and maintained in acpPC, we might expect that the disassembly occurring during IEC processing should have minimal stripping effects on the central Chl c_2. The Chl *a* and diadinoxanthin molecules located on the peripheral regions of acpPC and thus on the interfaces between acpPC subunits of an oligomeric acpPC, however, tend to be easily lost. Indeed, the difference spectrum (Fig. 2a, black dash-dot) could be very well mimicked by a sum of the individual 77 K absorption spectra of Chl *a* (green) and diadinoxanthin (orange) recorded in 2-methyltetrahydrofuran (2-MTHF), adequately shifted to match their peak positions. It confirms that upon further purification and subsequent concentration of oligomeric acpPC, some fractions of peripherally-bound Chl *a* and diadinoxanthin were permanently lost from the protein structure. For reference, the 77 K absorption spectrum of a previously studied acpPC trimer was also added for comparison (Jiang et al. 2014; Niedzwiedzki et al. 2014). This spectrum was intuitively normalized with that of the SDG-IEC-acpPC at 510 nm, upon an assumption that absorbance of the latter should not overpass the former at any wavelength. The spectral shape clearly reveals that the trimeric acpPC lacks a substantial pool of Chls *a* and carotenoids from its structure compared to the nonameric acpPC (Fig. 2b, green line and orange line). Consequently, even at this point, we might hypothesize that migration of the excitation energy within the nonamer and previously purified acpPC trimer could be substantially altered.

Although the absorption spectra of all the acpPC complexes show the Q_y band of Chl *a* at 671 nm, major differences between the trimeric acpPC and SDG- and SDG-IEC-acpPC are clearly observed in the fluorescence emission spectra (Fig. 2b). Note, these spectra, normalized for better comparability, were obtained by time-integration of time-resolved fluorescence profiles, which are provided in the next section. The spectra show that partial loss of Chl *a* and diadinoxanthin in SDG-IEF-acpPC does not cause substantial alterations of the emission band with respect to SDG-acpPC, probably because major population of Chls *a* associated with emission still remains intact. Although some peak shifting/narrowing in the SDG-IEC-acpPC profile is noticeable (Fig. 2b). The differences between these two acpPC complexes and the trimeric acpPC are substantial. The fluorescence emission spectrum of the trimeric acpPC is narrower and its maximum is shifted to shorter wavelength (from 685–688 nm to 676 nm).

Spectral reconstruction of absorption spectrum and determination of pigment stoichiometry

The absorption difference profile (Fig. 2a) can be adequately mimicked by the sum of the individual 77 K absorption spectra of Chl *a* and diadinoxanthin. This makes the spectral reconstruction of the main absorption band (400–600 nm) of the SDG-acpPC absorption spectrum feasible—those will be approximated positions of the absorption spectra of two classes of pigments bound to the complex. The attempt is demonstrated in Fig. 3a. The absorption spectra of each individual pigments recorded at 77 K in 2-MTHF were used, with their spectra shifted to optimal positions and adjusted in amplitudes for the best agreement. Note that in all cases, two different spectral forms were necessary for proper spectral modelling. The reconstructed vs. the experimental spectra do match well except in the 400–430 nm spectral range, suggesting that the amplitudes of the B bands in the Chl *a* absorption spectrum can be elevated if the pigment is buried into the complex. In addition, a small energetic spacing between the absorption spectra of diadinoxanthin may suggest that in acpPC, the carotenoid is represented by just one spectral form with broader vibronic bands, possibly due to the protein-driven geometric distortion of the conjugated part of the molecule, which, however, is not the case in the 2-MTHF glass.

The pigment stoichiometry in the SDG-acpPC was calculated based on the spectral reconstruction of the methanol extracts of the complex using the absorption spectra of each individual pigments recorded in methanol (Fig. 3b). The detailed procedure is provided in the Supplementary Information and in Fig S2. Our estimate gives Chl *a*:Chl c_2:Per:Diad pigment stoichiometry of 8:6:11:3. It is informative to put it in the context of the pigment contents of the light-harvesting complexes (monomers) for which the crystal structures are known. Therefore, for FCP from diatom Chl *a*:Chl c_2:Cars is 7:2:7 and for major LHCII from plants, Chl *a*:Chl *b*:Cars is 8:6:4 (Cars – collective carotenoids) (Liu et al. 2004; Wang et al. 2019). If the theme of 7–8 Chl *a* per complex monomer is consistent across the whole protein superfamily, we might hypothesize that the fully intact acpPC will bind 8 Chl *a*, 6 Chl c_2, 11 Per and 3 Diad. On the other hand, considering that the overall number of carotenoids bound to antenna ranges from 4 to 7, the estimate provided above should be divided by a factor of 2 to give a better agreement. Considering the difference in absorption spectra of SDG- and SDG-IEC-acpPC complexes (Fig. 2a) and spectrum reconstruction of SDG-acpPC (Fig. 3a), it seems that further purification and processing of the complex causes 15–20% losses of Chl *a* and diadinoxanthin.

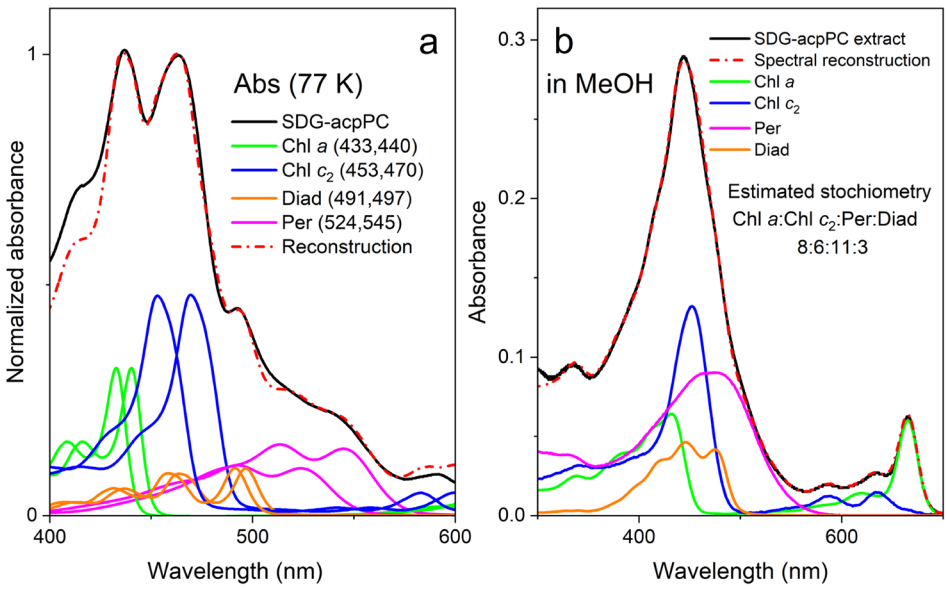

Fig. 3 Spectral reconstruction of the absorption spectra of SDG-acpPC and its solvent extract. **a** Spectral reconstruction of 77 K absorption spectrum of SDG-acpPC with the absorption spectra of each individual pigment taken at 77 K in 2-MTHF and adequately shifted. For Chls, position of the Soret band and for carotenoids, position of the (0–0) vibronic band is provided. **b** Spectral reconstruction of absorption spectrum of methanol extract of SDG-acpPC with absorption spectra of individual pigments taken in methanol. This analysis provides the estimated pigment stoichiometry in the complex. For more details on the procedure refer to SI

Time-resolved fluorescence imaging

The temporal characteristics of the fluorescence emission decay of Chl *a* in both SDG-acpPC and SDG-IEC-acpPC were investigated at 77 K. Previous 77 K time-resolved fluorescence analysis on the trimeric acpPC from the same organism demonstrated that, upon excitation of the carotenoid band, the excitation energy is promptly transferred to Chls and subsequently emitted as Chl *a* fluorescence. It is characterized by a single exponential component decay with a lifetime of 5.8 ns. No other kinetic components were revealed in the fluorescence decay profile (Niedzwiedzki et al. 2014). However, a very different scenario was observed in both SDG- and SDG-IEC-acpPC. Figure 4 presents the time-resolved fluorescence (TRF) imaging and subsequent spectro-temporal global analysis. The TRF images were recorded using very low excitation intensity at 540 nm, the spectral range that mostly coincides with the absorption band of acpPC-bound peridinin (Polivka et al. 2006, Niedzwiedzki et al. 2014). It is known that upon direct excitation of peridinin in acpPC, the excitation is promptly and efficiently transferred to Chl *a*. Therefore, this selection of excitation wavelength warrants that the entire Chl *a* fluorescence emission is associated with the protein-bound Chls *a*. The TRF decay images of the SDG-acpPC and SDG-IEC-acpPC (Fig. 4a, b) clearly reveal more complex features than those previously reported for the trimeric acpPC, but subtle differences also exist between the two preparations (SDG-acpPC and SDG-IEC-acpPC). Detailed information on the fluorescence emission dynamics can be achieved by performing global analysis of the TRF datasets (van Stokkum et al. 2004). The outcomes of our fitting are provided in Fig. 4c, d. The data modelling was done according to the kinetic schemes provided in the figure insets. Hypothetically, the model should account for the fact that upon excitation at 540 nm (peridinin), excitation energy is transferred to Chl *a* collectively from the carotenoid singlet excited S_2 and S_1 states. This process corresponds to the rise of Chl *a* fluorescence emission. However, as such process occurs in an ultrafast time regime (a few picoseconds) (Polivka et al. 2006, Niedzwiedzki et al. 2014), the spectra cannot be temporally resolved due to the TRF technical setup limitations. Therefore, an applied fitting model to the experimental data must assume that the excitation directly populates/excites the first spectro-temporal fluorescence component detectable in the data, which is already associated with Chl *a*. Overall, three spectro-temporal components were required to successfully model the TRF decay images in both cases. Because the data modelling was based on anticipated or so-called target model, the results were called species associated fluorescence spectra (SAFS) and were denoted as F682, F687 and F695/698, based on approximate positions of their maxima expressed in nanometers. The first two SAFS also have competing intrinsic decays to the ground state fixed at 5.8 ns, which corresponds to the intrinsic decay of excited monomeric Chl *a* in the trimeric acpPC (Niedzwiedzki et al. 2014; Vinklarek et al. 2018). It could be interpreted that it is as if the oligomer falls apart into trimers, such that the various spectral species of Chl *a* will be reduced to one with a fluorescence lifetime of 5.8 ns (at 77 K).

The SAFS were also corrected for their time dependent concentration in the TRF profile by multiplying the amplitude profiles by the maximum of time dependent concentration, $C_{max}(t)$ (van Stokkum et al. 2004). This product more intuitively highlights the possible relative contributions of the components in the TRF data. The fitting demonstrates

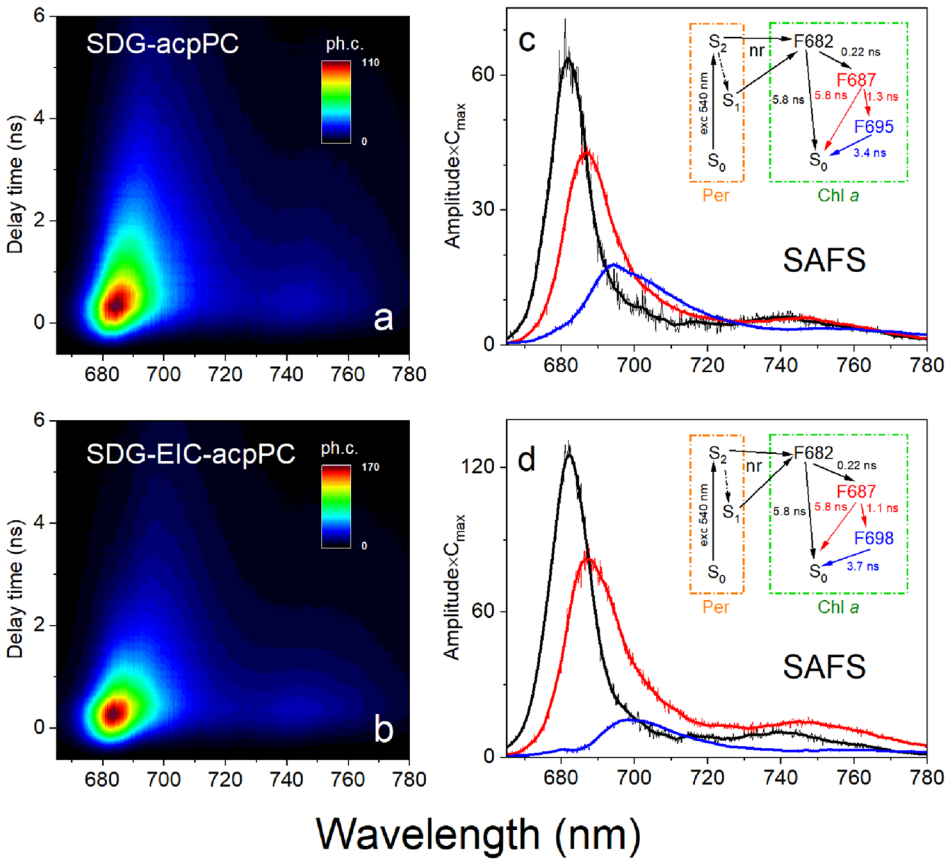

Fig. 4 77 K time-resolved fluorescence (TRF) decay imaging of oligomeric acpPC after SDG and SDG-IEC, respectively. The samples were excited at 540 nm (Per—peridinin). **a**, **b** 2D pseudo-color TRF profiles in which colors represent emission intensities (photon counts, ph. c.). **c**, **d** Global analysis of fluorescence emission decay profiles. Refer to the main text for more details. The profiles were smoothed for better clarity. *SAFS*—species associated fluorescence spectra (smoothed for clarity), *nr*—not resolved, *F682–F698*—various Chl *a* fluorescence species

that there are three distinct Chl *a* spectral forms (Fig. 4c, d). Once the excitation enters the Chl *a* network, it is very quickly transferred to the more red-emissive pigments and ultimately trapped in the Chl *a* pool with fluorescence emission maximum at ~ 700 nm, which finally decays to the ground state. The dynamics of this process is very similar in both oligomeric forms of acpPC (SDG and SDG-IEC) though it is evident that the SDG sample has noticeably larger contributions of the energetically lowest (most red-shifted) fluorescence component. It strongly suggests that the further purification step performed after SDG alters the energetic landscape of the protein-bound Chls or it might be correlated with the observed ~ 10% loss of Chl *a* during post-SDG purification. Since SDG-IEC-acpPC is an ensemble with a large range of oligomerization extent (Fig. 1b), the numerical treatment of it is basically averaged. Another note is that even though fluorescence decay shows different spectral species, these spectral forms of Chl *a* are not clearly manifested in the absorption spectrum in both samples.

Transient absorption

Time-resolved fluorescence imaging data provide useful information of Chl *a* fluorescence dynamics. This method, however, does not resolve early events after excitation due to its low temporal resolution. Since TRF measurement only monitors light emission, it cannot characterize possible non-emitting states, which may concurrently form during the excitation migration within the acpPC oligomeric assembly. To address this issue, both SDG- and SDG-IEC-acpPC were subjected to further study using femtosecond time-resolved transient absorption spectroscopy. The data were collected at both room temperature (RT) and 77 K, upon excitation at 540 nm (comparable to TRF). Considering the spectral reconstruction of the absorption spectrum of SDG -acpPC shown in Fig. 3a, that wavelength should essentially exclusively excite peridinin and the spectral evolution observed in the TA profile is associated with excitation energy migration from peridinin excited states (S_2 and S_1) to Chls. The data modeling is shown in Fig. 5 (for exemplary raw TA spectra refer to Fig. S3), and assumes that peridinin (Per) is excited to S_2 state. The intrinsic lifetime of carotenoid S_2 state ranges between 100 and 300 fs (Polivka and Sundstrom 2004). For simplicity, we used the low-end value for peridinin. If the carotenoid is not energetically coupled to its neighboring Chl *a* or Chl c_2 molecules, the excited S_2 state will internally convert to the S_1 state that subsequently will intrinsically decay to the ground state with a lifetime of 11 ps (peridinin, average S_1 state lifetime in polar solvent) (Bautista et al. 1999; Zigmantas et al. 2001; Zigmantas et al.

2003). Again, for simplicity, it was assumed that peridinin S_1 and S_2 states lifetimes are also temperature independent. TA data modeling assumes that the S_2 state will be efficiently transferring excitation to both types of Chls. However, the carotenoid S_1 state is more fit to transfer excitation energy to Chl *a* due to a better overlap of peridinin fluorescence emission and Q_y absorption band of Chl *a*. Because we cannot temporally resolve excitation transfer from peridinin S_2 state to both Chl c_2 and *a*, we assumed that the time constants are 100 fs, comparable to the state lifetime. The time constant for the S_1 state-related excitation migration route was then estimated at 0.9 ps. Modeling demonstrated that Chl c_2 efficiently transfer excitation to Chl *a* with a time constant of 5.4 ps. As is in this case, a customized fitting model is applied to TA datasets, and the fitting results are commonly called species associated difference spectra (SADS) (van Stokkum et al. 2004). If a model sufficiently mimics the realistic pathways of the excitation migration/decay, SADS should very closely correspond to the spectral features (ground state absorption bleaching (GSB) with accompanied excited state absorption band (ESA)) of individual pigments.

Closer inspection of SADS shows that the profiles fulfill those criteria particularly for RT TA data. The green SADS, associated with the S_2 state of peridinin, clearly consists of bleaching of the ground state absorption accompanied with a positive band which, based on the previous studies of a few variants of acpPC complex or peridinin-only PCP, corresponds to peridinin $S_2 \rightarrow S_n$ ESA band. The red SADS corresponds to the S_1 state of peridinin and consists of bleaching of steady-state absorption and adjacent $S_2 \rightarrow S_n$ ESA (Ilagan et al. 2006, Polivka et al. 2006, Schulte et al. 2009a, b, van Stokkum et al. 2009, Niedzwiedzki et al. 2013, Slouf et al. 2013, Niedzwiedzki et al. 2014). The black SADS is associated with Chl c_2. The negative part very adequately corresponds to the bleaching of the Soret band and is accompanied by the broad positive ESA, which surpasses the expected bleaching of the Q_y band at ~ 650 nm (Niedzwiedzki et al. 2014). The blue SADS is associated with a pool of excited Chls *a* populated via excitation energy

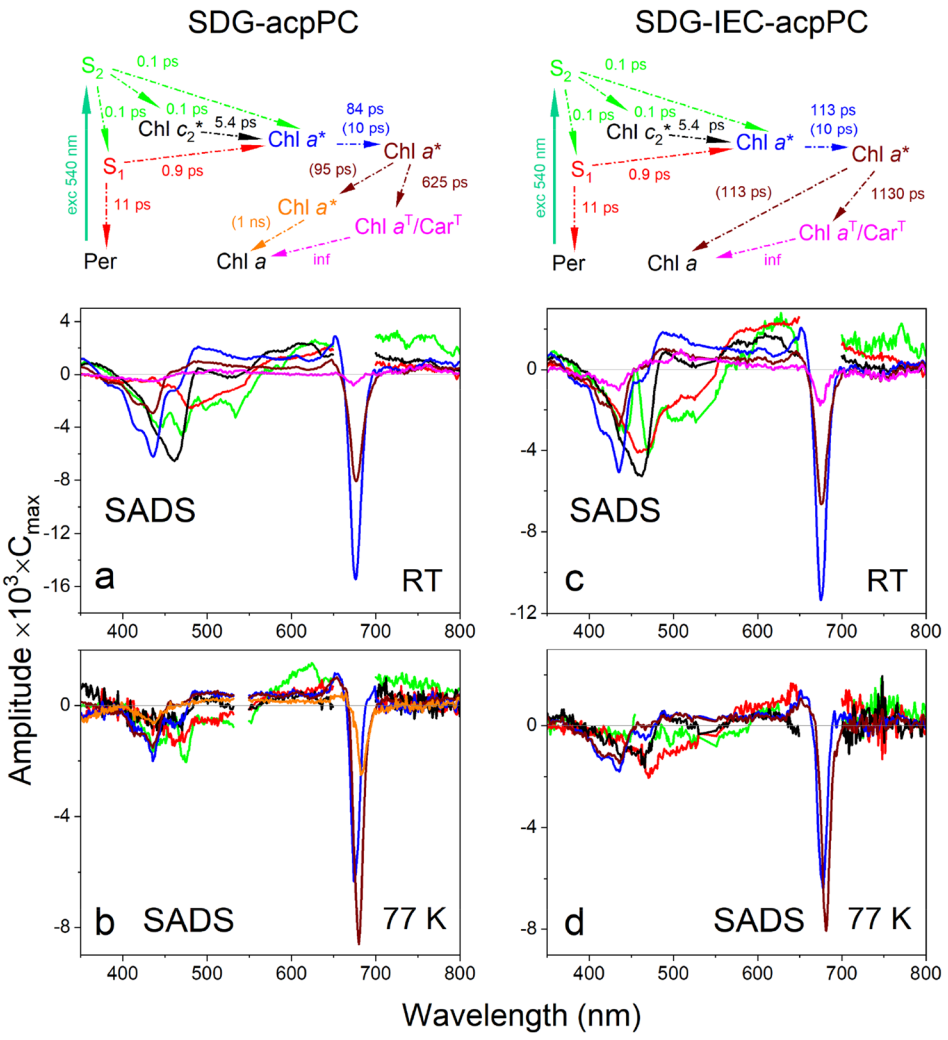

Fig. 5 Global analysis of TA datasets of **a**, **b** SDG-acpPC and **c**, **d** SDG-IEC-acpPC preparations performed according to anticipated models of excitation migration pathways presented in the above graphs. It was assumed that excitation at 540 nm will initially promote peridinin (Per) to its S_2 excited singlet state. Subsequently, excitation energy quickly funnels to Chls *a* directly or via Chl c_2. Modelling demonstrated that the last stage of the excitation migration pathway alternates at cryogenic temperature. Refer to the main text for more details. Time constants in parentheses (and associated routes) are for 77 K. *SADS*—species associated decay spectrum, *Car*—carotenoid (peridinin and/or diadinoxanthin), *—excited states

transfer from peridinin and Chl c_2. This SADS, associated with excited Chls *a*, quickly evolves with a time constant of 84–113 ps to another Chl *a*-related component (brown SADS). At RT, these two SADS are essentially identical in shapes, but the latter has a substantially smaller contribution in the TA datasets (SADS were corrected for their maximal time dependent concentration). Instead of being associated with the energetic equilibration of the excited pigment (otherwise, SADS amplitudes should not change but rather shift in position), the 84–113 ps time constant is associated with the depletion of the TA signal, most likely due to singlet–singlet annihilation.

A final pool of the excited Chls (brown SADS) decays with an observed lifetime of 625–1130 ps. These time constants are substantially shorter than the Chl *a* fluorescence lifetime recorded for the trimeric acpPC (Chl *a* monomers), which strongly supports the idea of an oligomerization-driven singlet–singlet annihilation. The elongated Chl *a* fluorescence dynamics in SDG-IEC-acpPC in regard to SDG-acpPC and the same elongated time constants in SDG-IEC-acpPC indicates that additional sample processing progressively disrupts the native oligomerization state of the complex and consequently reduces the probability of the annihilation process occurring between the excited Chls, which are most likely located somewhere at stitching interfaces between each individual trimers in the oligomer. Efficient singlet–singlet annihilation of the excited Chl *a* observed even at low excitation intensities (shortening of the Chl *a* fluorescence lifetime) can maximally reduce the chance of formation of Chl *a* triplets and subsequent sensitization of carotenoid (peridinin/diadinoxanthin) triplets. This is clearly demonstrated for the SDG-acpPC sample, where the combined signals with Chl *a* and carotenoid triplets were barely seen (magenta SADS). However, once the aggregation level of acpPC changes and the lifetime of the longer-lived Chl *a* subsequently elongates, the population of Chl *a*/carotenoid triplets grows (compare magenta SADS in Fig. 5a and c). Notable difference induced at 77 K is that the acpPC oligomers do not reveal any detectable accumulation of Chl *a*/peridinin triplets (no magenta SADS). The dynamics of the excited singlet state of Chl *a* is also altered. Overall, it is substantially faster and reduces formation of Chl *a* triplets.

At this point, the TRF and TA analysis have given some complementary characteristics of the excited Chls *a* at 77 K. In summary, for the SDG-acpPC sample, both TA and TRF fitting data have revealed that there are three spectro-kinetic components associated with Chl *a*. Considering that the TA lifetime results support that the excited Chls may be additionally affected by excitation annihilation, the following conclusions can be reached. The F682 SAFS component parallels the blue SADS with the observed bleaching of the Q_y band at 676 nm. The F687 SAFS corresponds to the brown SADS with the observed bleaching of the Q_y band at 681 nm, and the F695 SAFS would correspond to the orange SADS with the observed bleaching of the Q_y band at 684 nm. Note that it is still misleading to directly match the SAFS to the SADS components in terms of the positions of their fluorescence maxima and bleaching minima (e.g., F682 SAFS and 681 nm SADS) *a*. In the TA spectrum, the observed "bleaching" of the Chl *a* Q_y band corresponds to a collective signals of the real bleaching of the Q_y absorption band and the probe-driven stimulated emission (fluorescence emission). Since the detector unfortunately does not have the resolution of discriminating between them (due to the nature of the instrumental setting), the recorded "bleaching" band simply represents a combination of both, and a collective peak is detected, with a minimum located around halfway between the maxima of the absorption band and the fluorescence emission.

Discussion

Our purification and biochemical characterizations of the acpPC complexes from a dinoflagellate *Fugacium kawagutii* in this study illustrates that higher-order structural organizations of the acpPC antenna complex can be kept intact and isolated if appropriate buffers and purification protocols are followed. All these rely on the use of high molarity of betaine in the preparation buffers, which has been successfully used for reaction centers isolation in multiple organisms. It should be noted that the higher-order oligomeric structure of acpPC can be disrupted and reassembled in *in vitro* experiments, resulting in a heterogenous mixture (SDG-IEC) (Fig. 1b, right panel). Spectroscopically, they are not exactly the same as the original nonameric form (SDG). It seems that single-step SDG ultracentrifugation (without extensive chromatography) represents a much milder isolation strategy that keeps the protein complex in its native-like state and relatively high purity (Fig. 1c). The pigment composition analysis of SDG-acpPC of SDG-IEC-acpPC indicates that further biochemical processing (adsorption to the chromatography resin and washing in the presence of detergents that have to be included in the reagent buffers) tends to reduce the pigment content. At present time, there are no 3D structural data from either protein X-ray crystallography or cryo-EM studie, we do not know where and how the (stripped) pigments may have interacted with the apo-protein in nonameric acpPC or with the other cofactors in the complex. Hydrophobic interactions in LHC are usually the major force stabilizing the pigments and their associated binding partners, such as membrane lipids. The more native lipids the protein samples retain, the more pigments are found stabilized in the biochemical preparations (Buchel 2003; Beer et al. 2006; Lepetit et al. 2010). Apparently, extensive exposure of the solubilized samples to the

detergents which are necessarily used in the biochemical buffers during IEC will inevitably strip off those loosely bound pigments. Those pigments may be located either on the surface of the acpPC nonamer or the interfaces between each subunit in the oligomer. Previously, it has been reported that in the FMO antenna complex containing bacteriochlorophyll *a* (BChl *a*), the eighth BChl *a* pigment, located in the interface of trimeric FMO, can be easily lost during purification owing to surface exposure (Wen et al. 2011). Here, we could reasonably suspect a similar situation could occur for the nonameric acpPC. Please note, the eighth pigment discovery in FMO had a huge impact on the excitation energy research in the community. We highly recommend our SDG method for future acpPC and its relevant research studies. Based on findings presented in this study, the overall picture is that the native acpPC is predominantly clustered to larger acpPC oligomers, most likely trimer of trimers (nonamer), acpPC$^{(3\times3)}$.

Previous time-resolved fluorescence analysis on oligomers of the major LHC in higher plants indicated that the oligomerized LHC trimers tend to form a weakly-coupled inter-trimer Chl *a*-Chl *a* excitation state. They are characterized by a strongly far-red enhanced fluorescence spectrum, strikingly similar to the fluorescence component observed in intact leaves when NPQ is induced (Miloslavina et al. 2008). Our time-resolved spectroscopic studies on the oligomeric acpPC in this research show similar Chl *a* fluorescence characteristics as observed in higher plants. A very interesting question that immediately arises is how this acpPC oligomer interacts with RCs, such as photosystem II (PSII). Unfortunately, the modified purification protocol is still not adequate for successful separation of PSII, most likely because the photosystems are extremely fragile and fall apart even during ever-known gentle detergent treatment of the thylakoid membrane. Another interesting aspect is how such oligomeric representation of acpPC (nonamer) is natively preferred. Uncoincidentally, recent structural determinations on more intact algal PSII-LHCII supercomplex showed that the major LHC complex forms closely associated trimer of LHCII trimers, i.e., nonamer, which is then coupled to the photosystem core complex via minor light-harvesting CP29 complex (Burton-Smith et al. 2019; Shen et al. 2019).

Spectroscopically, the nonameric acpPC is substantially different than its trimeric counterpart. The differences are readily seen in steady-state absorption and fluorescence emission spectra at 77 K. The most interesting findings, however, come from the completely different dynamics of the excited states of the acpPC-bound Chls *a* among the oligomeric and trimeric acpPC. Previous work showed that in acpPC trimer, the excited Chl *a* is uniform and has one spectral form with a mono-exponential component decay with a lifetime of ~ 5.8 ns (at 77 K) (Niedzwiedzki et al. 2014). Those studies showed that the acpPC trimer is spectroscopically very homogenous without any spectral heterogeneity that could benefit the excitation migration downhill to a specific site in the trimer assembly. This picture is completely altered in the more native oligomeric assembly studied in this work. The fluorescence components with red-shifted emission peaks may represent a characteristic marker for NPQ condition in *Symbiodiniaceae* cells under photoprotection model. The time-resolved fluorescence and transient absorption studies also demonstrated the presence of three spectrally and dynamically different forms of excited Chl *a*. Excitation dynamics of these pigments show that excitation very likely spatially migrates within the oligomer to a specific site due to unidirectional energetic funneling from the energetically highest to lowest Chls. Hypothetically, it is possible that this mechanism somehow maneuvers excitations from photons absorbed in random places within the oligomeric assembly into a specific location that could ultimately transfer it to the adjacent PSII access point or to a non-photochemical quenching center if hopping of excitation to PSII is not possible (or a closed PSII). Research on the NPQ candidate proteins in this species is underway.

Supplementary Information The online version contains supplementary material available at https://doi.org/10.1007/s11120-022-00951-6.

Acknowledgements The authors thank Atsuko Kanazawa in David Kramer's lab for sharing the *Fugacium kawagutii* strain and helpful discussion. D.N.M. acknowledges Center for Solar Energy and Energy Storage at McKelvey School of Engineering at Washington University in Saint Louis for finanacial support. N.C. M. M. was supported by the U.S. Department of Energy (DOE), Office of Basic Energy Sciences under grant DE-CD0002036 to Professors: Chris Kirmaier and Dewey Holten. This research was supported by the Danforth Seed Grant of Department of Biology at Washington University in Saint Louis (to H.L.). H. L. also acknowledges the U.S. Department of Energy (DOE), Office of Basic Energy Sciences, Photosynthetic Systems (PS) Program (Grant DE-FG02-07ER15902 to H.L.).

Funding This study was supported by U.S. Department of Energy (Grant No. DE-FG02-07ER15902, DE-CD0002036), and Danforth Foundation, Seed grant Biology Washington University.

Declarations

Conflict of interest The authors have no competing interests to declare that are relevant to the content of this article.

References

Bautista JA, Connors RE, Raju BB, Hiller RG, Sharples FP, Gosztola D, Wasielewski MR, Frank HA (1999) Excited state properties of peridinin: observation of a solvent dependence of the lowest excited singlet state lifetime and spectral behavior unique among carotenoids. J Phys Chem B 103(41):8751–8758

Beer A, Gundermann K, Beckmann J, Buchel C (2006) Subunit composition and pigmentation of fucoxanthin-chlorophyll proteins in diatoms: evidence for a subunit involved in diadinoxanthin and diatoxanthin binding. Biochemistry 45(43):13046–13053

Blankenship RE (2021) Molecular Mechanisms of Photosynthesis, pp. 61-87. (John Wiley & Sons).

Buchel C (2003) Fucoxanthin-chlorophyll proteins in diatoms: 18 and 19 kDa subunits assemble into different oligomeric states. Biochemistry 42(44):13027–13034

Buchel C (2015) Evolution and function of light harvesting proteins. J Plant Physiol 172:62–75

Burton-Smith RN, Watanabe A, Tokutse R, Song CH, Murata K, Minagawa J (2019) Structural determination of the large photosystem II?light-harvesting complex II supercomplex of *Chlamydomonas reinhardtii* using nonionic amphipol. J Biol Chem 294(41):15003–15013

Di Valentin M, Salvadori E, Agostini G, Biasibetti F, Ceola S, Hiller R, Giacometti GM, Carbonera D (2010) Triplet-triplet energy transfer in the major intrinsic light-harvesting complex of *Amphidinium carterae* as revealed by ODMR and EPR spectroscopies. BBA-Bioenergetics 1797(10):1759–1767

Durnford DG, Deane JA, Tan S, McFadden GI, Gantt E, Green BR (1999) A phylogenetic assessment of the eukaryotic light-harvesting antenna proteins, with implications for plastid evolution. J Mol Evol 48(1):59–68

Hiller RG, Wrench PM, Gooley AP, Shoebridge G, Breton J (1993) The major intrinsic light-harvesting protein of *Amphidinium* - characterization and relation to other light-harvesting proteins. Photochem Photobiol 57(1):125–131

Hiller RG, Wrench PM, Sharples FP (1995) The light-harvesting chlorophyll *a-c*-binding protein of dinoflagellates—a putative polyprotein. FEBS Lett 363(1–2):175–178

Hofmann E, Wrench PM, Sharples FP, Hiller RG, Welte W, Diederichs K (1996) Structural basis of light harvesting by carotenoids: peridinin-chlorophyll-protein from *Amphidinium carterae*. Science 272(5269):1788–1791

Iglesiasprieto R, Govind NS, Trench RK (1991) Apoprotein composition and spectroscopic characterization of the water-soluble peridinin chlorophyll alpha-proteins from 3 symbiotic dinoflagellates. Proc R Soc B-Biol Sci 246(1317):275–283

Ilagan RP, Koscielecki JF, Hiller RG, Sharples FP, Gibson GN, Birge RR, Frank HA (2006) Femtosecond time-resolved absorption spectroscopy of main-form and high-salt peridinin-chlorophyll *a*-proteins at low temperatures. Biochemistry 45:14052–14063

Jiang J, Zhang H, Orf GS, Lu Y, Xu W, Harrington LB, Liu H, Lo CS, Blankenship RE (2014) Evidence of functional trimeric chlorophyll a/c2-peridinin proteins in the dinoflagellate *Symbiodinium*. Biochim Biophys Acta 1837(11):1904–1912

Kanazawa A, Blanchard GJ, Szabo M, Ralph PJ, Kramer DM (2014) The site of regulation of light capture in *Symbiodinium*: does the peridinin-chlorophyll a-protein detach to regulate light capture? Biochim Biophys Acta 1837(8):1227–1234

Lepetit B, Volke D, Gilbert M, Wilhelm C, Goss R (2010) Evidence for the existence of one antenna-associated, lipid-dissolved and two protein-bound pools of diadinoxanthin cycle pigments in diatoms. Plant Physiol 154(4):1905–1920

Liu ZF, Yan HC, Wang KB, Kuang TY, Zhang JP, Gui LL, An XM, Chang WR (2004) Crystal structure of spinach major light-harvesting complex at 2.72 angstrom resolution. Nature 428(6980):287–292

Miloslavina Y, Wehner A, Lambrev PH, Wientjes E, Reus M, Garab G, Croce R, Holzwarth AR (2008) Far-red fluorescence: a direct spectroscopic marker for LHCII oligomer formation in non-photochemical quenching. FEBS Lett 582(25–26):3625–3631

Niedzwiedzki DM, Fuciman M, Frank HA, Blankenship RE (2011) Energy transfer in an LH4-like light harvesting complex from the aerobic purple photosynthetic bacterium *Roseobacter denitrificans*. Biochem Biophys Acta 1807(5):518–528

Niedzwiedzki DM, Jiang J, Lo CS, Blankenship RE (2013) Low-temperature spectroscopic properties of the peridinin-chlorophyll a-protein (PCP) complex from the coral symbiotic dinoflagellate *Symbiodinium*. J Phys Chem B 117(38):11091–11099

Niedzwiedzki DM, Jiang J, Lo CS, Blankenship RE (2014) Spectroscopic properties of the chlorophyll a-chlorophyll c (2)-peridinin-protein-complex (acpPC) from the coral symbiotic dinoflagellate *Symbiodinium*. Photosynth Res 120(1–2):125–139

Polivka T, Sundstrom V (2004) Ultrafast dynamics of carotenoid excited states—from solution to natural and artificial systems. Chem Rev 104(4):2021–2071

Polivka T, van Stokkum IH, Zigmantas D, van Grondelle R, Sundstrom V, Hiller RG (2006) Energy transfer in the major intrinsic light-harvesting complex from *Amphidinium carterae*. Biochemistry 45(28):8516–8526

Reynolds JM, Bruns BU, Fitt WK, Schmidt GW (2008) Enhanced photoprotection pathways in symbiotic dinoflagellates of shallow-water corals and other cnidarians. Proc Natl Acad Sci U S A 105(36):13674–13678

Schagger H, von Jagow G (1991) Blue native electrophoresis for isolation of membrane protein complexes in enzymatically active form. Anal Biochem 199(2):223–231

Schulte T, Niedzwiedzki DM, Birge RR, Hiller RG, Polivka T, Hofmann E, Frank HA (2009a) Identification of a single peridinin sensing Chl-a excitation in reconstituted PCP by crystallography and spectroscopy. Proc Natl Acad Sci USA 106(49):20764–20769

Schulte T, Sharples FP, Hiller RG, Hofmann E (2009b) X-ray structure of the high-salt form of the peridinin-chlorophyll *a*-protein from the dinoflagellate *Amphidinium carterae*: Modulation of the spectral properties of pigments by the protein environment. Biochemistry 48(21):4466–4475

Schulte T, Johanning S, Hofmann E (2010) Structure and function of native and refolded peridinin-chlorophyll-proteins from dinoflagellates. Eur J Cell Biol 89(12):990–997

Sharples FP, Wrench PM, Ou KL, Hiller RG (1996) Two distinct forms of the peridinin-chlorophyll alpha-protein from *Amphidinium carterae*. BBA-Bioenergetics 1276(2):117–123

Shen LL, Huang ZH, Chang SH, Wang WD, Wang JF, Kuang TY, Han GY, Shen JR, Zhang X (2019) Structure of a C2S2M2N2 type PSII-LHCII supercomplex from the green alga *Chlamydomonas reinhardtii*. Proc Natl Acad Sci USA 116(42):21246–21255

Slouf V, Fuciman M, Johanning S, Hofmann E, Frank HA, Polivka T (2013) Low-temperature time-resolved spectroscopic study of the major light-harvesting complex of *Amphidinium carterae*. Photosynth Res 117(1–3):257–265

van Stokkum IH, Larsen DS, van Grondelle R (2004) Global and target analysis of time-resolved spectra. Biochim Biophys Acta 1657(2–3):82–104

van Stokkum IHM, Papagiannakis E, Vengris M, Salverda JM, Polivka T, Zigmantas D, Larsen DS, Lampoura SS, Hiller RG, van Grondelle R (2009) Inter-pigment interactions in the peridinin chlorophyll protein studied by global and target analysis of time resolved absorption spectra. Chem Phys 357(1–3):70–78

Vinklarek IS, Bornemann TLV, Lokstein H, Hofmann E, Alster J, Psencik J (2018) Temperature dependence of chlorophyll triplet quenching in two photosynthetic light-harvesting complexes from higher plants and dinoflagellates. J Phys Chem B 122(38):8834–8845

Wang WD, Yu LJ, Xu CZ, Tomizaki T, Zhao SH, Umena Y, Chen XB, Qin XC, Xin YY, Suga M, Han GY, Kuang TY, Shen JR (2019) Structural basis for blue-green light harvesting and energy dissipation in diatoms. Science 363(6427):598

Wen J, Zhang H, Gross ML, Blankenship RE (2011) Native electrospray mass spectrometry reveals the nature and stoichiometry of

pigments in the FMO photosynthetic antenna protein. Biochemistry 50(17):3502–3511
Zigmantas D, Polivka T, Hiller RG, Yartsev A, Sundstrom V (2001) Spectroscopic and dynamic properties of the peridinin lowest singlet excited states. J Phys Chem A 105(45):10296–10306
Zigmantas D, Hiller RG, Sundstrom V, Polivka T (2002) Carotenoid to chlorophyll energy transfer in the peridinin-chlorophyll-*a*-protein complex involves an intramolecular charge transfer state. Proc Natl Acad Sci USA 99(26):16760–16765
Zigmantas D, Hiller RG, Yartsev A, Sundstrom V, Polivka T (2003) Dynamics of excited states of the carotenoid peridinin in polar solvents: dependence on excitation wavelength, viscosity, and temperature. J Phys Chem B 107(22):5339–5348